Supporting Information

Multiferroic behavior between ferroelasticity and magnetization in two-dimensional organic-inorganic perovskites

Naoto Tsuchiya,[a] Saya Aoki,[a] Yuki Nakayama,[a] Goulven Cosquer,[bc] Sadafumi Nishihara,[abd] Miguel Pardo-Sainz,[ef] José Alberto Rodríguez-Velamazán,[g] Javier Campo[ce] and Katsuya Inoue*[abc]

[a]*Chemistry Program, Graduate School of Advanced Science and Engineering, Hiroshima University, 1-3-1 Kagamiyama, Higashi-Hiroshima, Hiroshima 739-8526, Japan*

[b]*Chirality Research Center (CResCent), Hiroshima University, 1-3-1 Kagamiyama, Higashi-Hiroshima, Hiroshima 739-8526, Japan*

[c]*International Institute for Sustainability with Knotted Chiral Meta Matter (WPI-SKCM^2), Hiroshima University, 1-3-1 Kagamiyama, Higashi-Hiroshima, Hiroshima 739-8526, Japan*

[d]*Precursory Research for Embryonic Science and Technology (PRESTO), Japan Science and Technology Agency (JST), 4-1-8, Honcho, Kawaguchi, Saitama 332-0012, Japan*

[e]*Aragón Nanoscience and Materials Institute (CSIC – University of Zaragoza) and Physics Condensed Matter Dept., C/Pedro Cerbuna 12, 50009 Zaragoza, Spain*

[f]*Graduate School of Science, Osaka Metropolitan University, 1-1, Gakuen-chou, Naka-ku, Sakai, Osaka 599-8531 Japan*

[g]*Institut Laue-Langevin, 71 avenue des Martyrs, CS 20156, 38042 Grenoble Cedex 9, France*

*Corresponding author: kxi@hiroshima-u.ac.jp

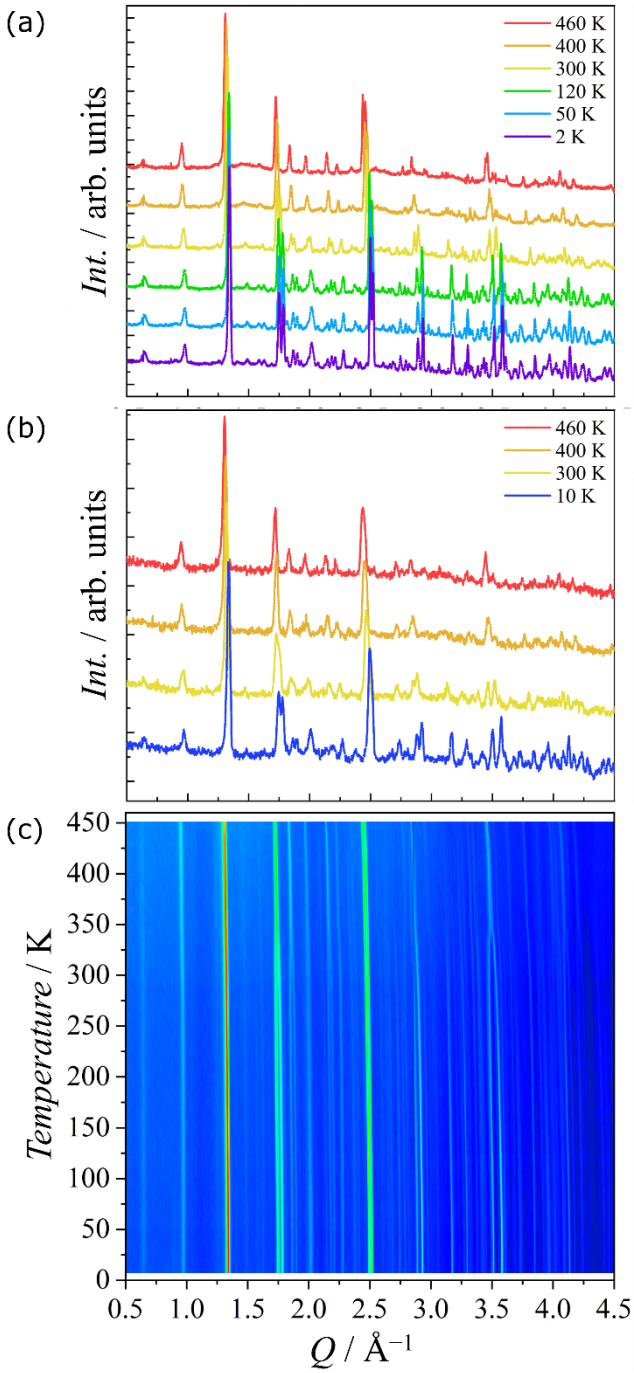

Fig. S1 (a) Raw diffractograms collected at D20 at fixed temperatures 2, 50, 120, 300, 400, and 460 K. (b) Raw diffractograms collected at D2B at fixed temperatures 10, 300, 400 and 460 K. (c) Warming up thermo-diffractograms collected at D20 from 2 K to 460 K.

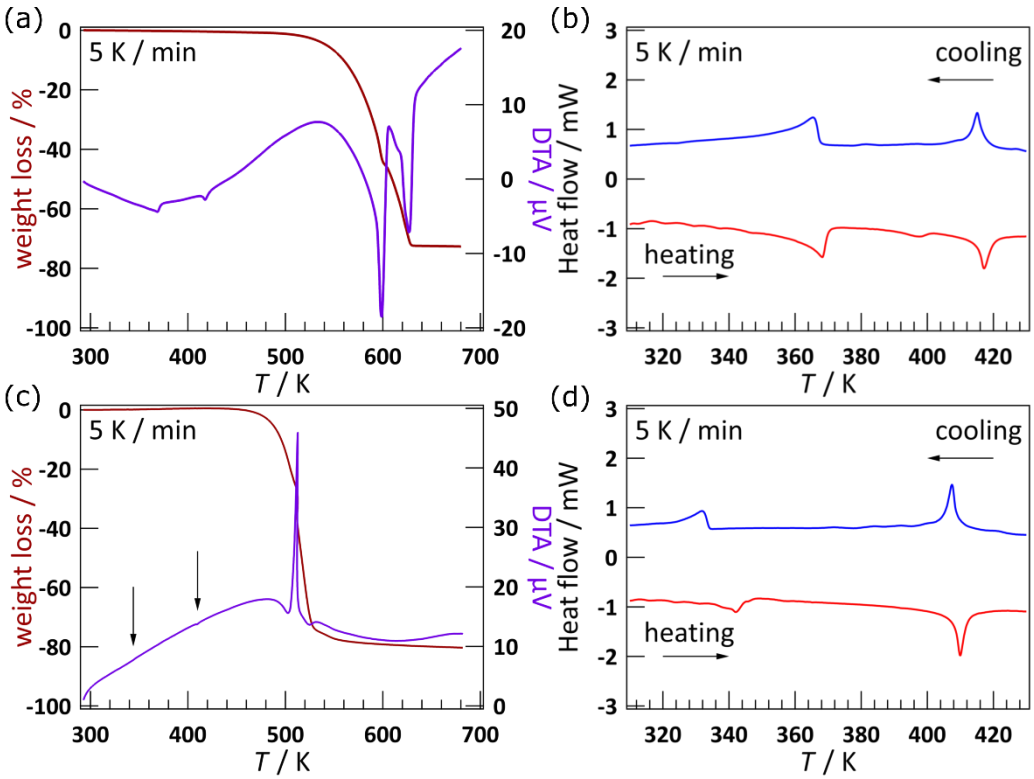

Fig. S2 (a, c) Thermal gravimetry (TG) measurements and differential thermal analysis (DTA) of (a) PEA-Mn and (c) PEA-Cu in the temperature range of 293 to 673 K. The arrows clarify the peak positions. (b, d) Differential scanning calorimetry (DSC) measurements of (b) PEA-Mn and (d) PEA-Cu.

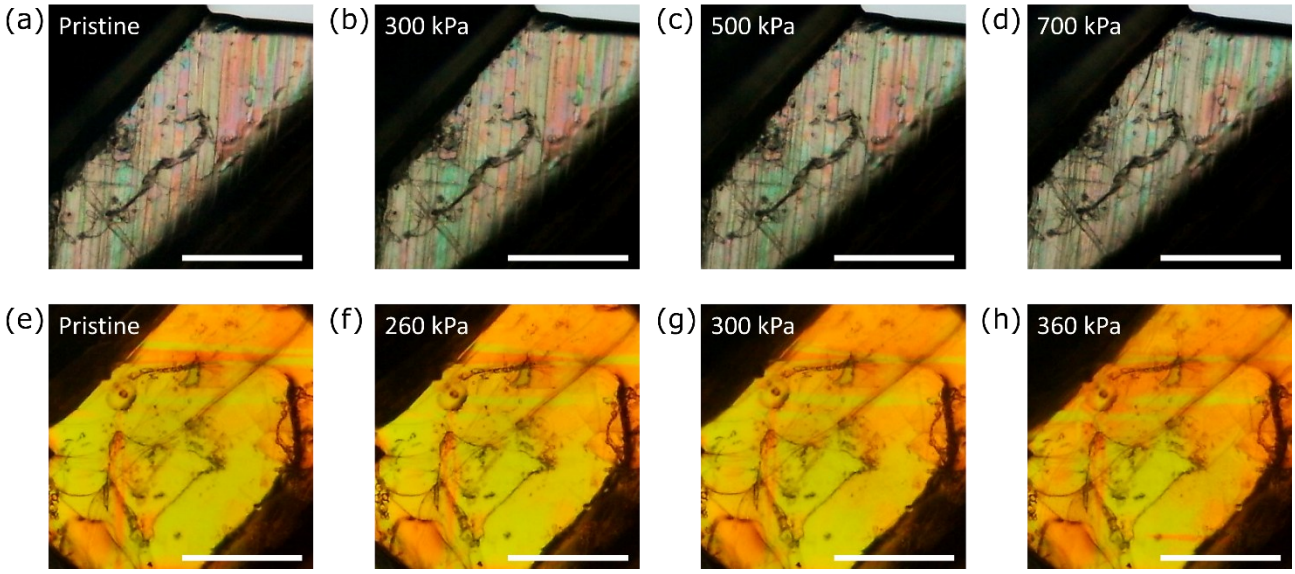

Fig. S3 Polarized microscopy observations of ferroelastic domains by applying mechanical stress for (a-d) PEA-Mn and (e-f) PEA-Cu. The changing in ferroelastic domains by external stress for (b-d) PEA-Mn and (f-h) PEA-Cu. The magnitude of the applied stress is indicated on each photo; scale bars = 0.5 mm.

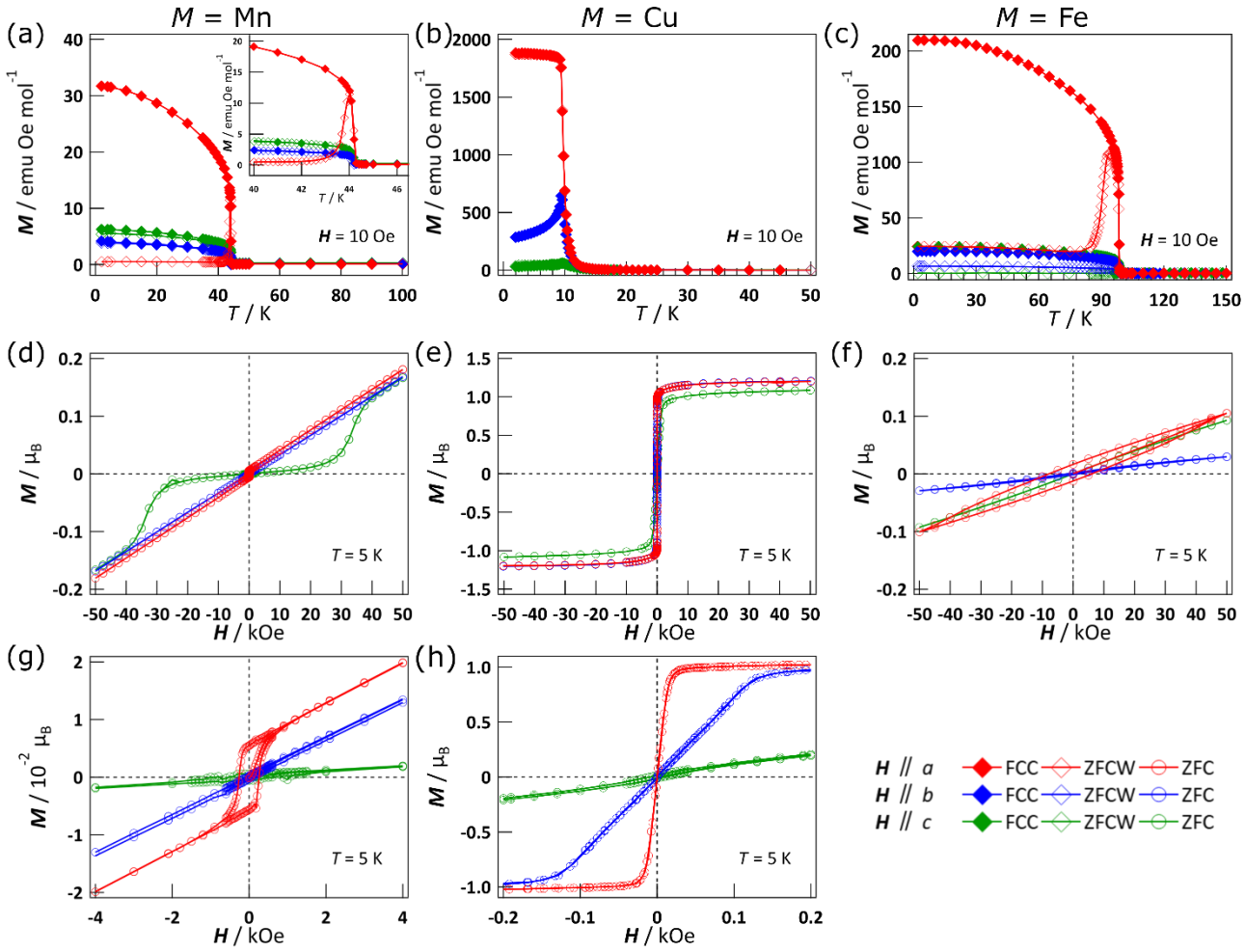

Fig. S4 (a-c) Temperature-dependence and (d-h) field-dependence of the magnetization for (a,d,g) PEA-Mn, (b,e,h) PEA-Cu and (c,f) PEA-Fe with magnetic field applied along the three crystallographic axes. Inset in figure (a) is a zoom around the T_N. Details in the magnetization versus magnetic field curves at low fields are shown in (g) and (h).

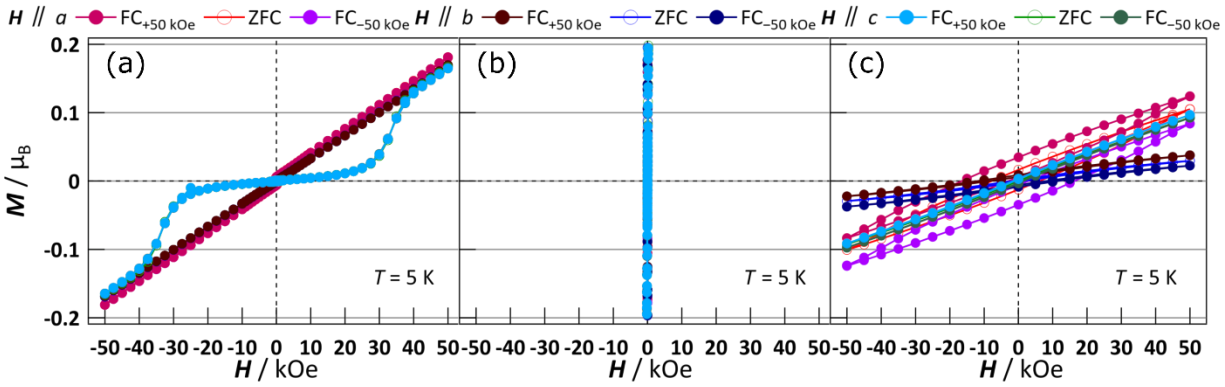

Fig. S5 Field-dependence of the magnetization for single crystals of (a) PEA-Mn, (b) PEA-Cu and (c) PEA-Fe in the range of ±0.2 μ_B.

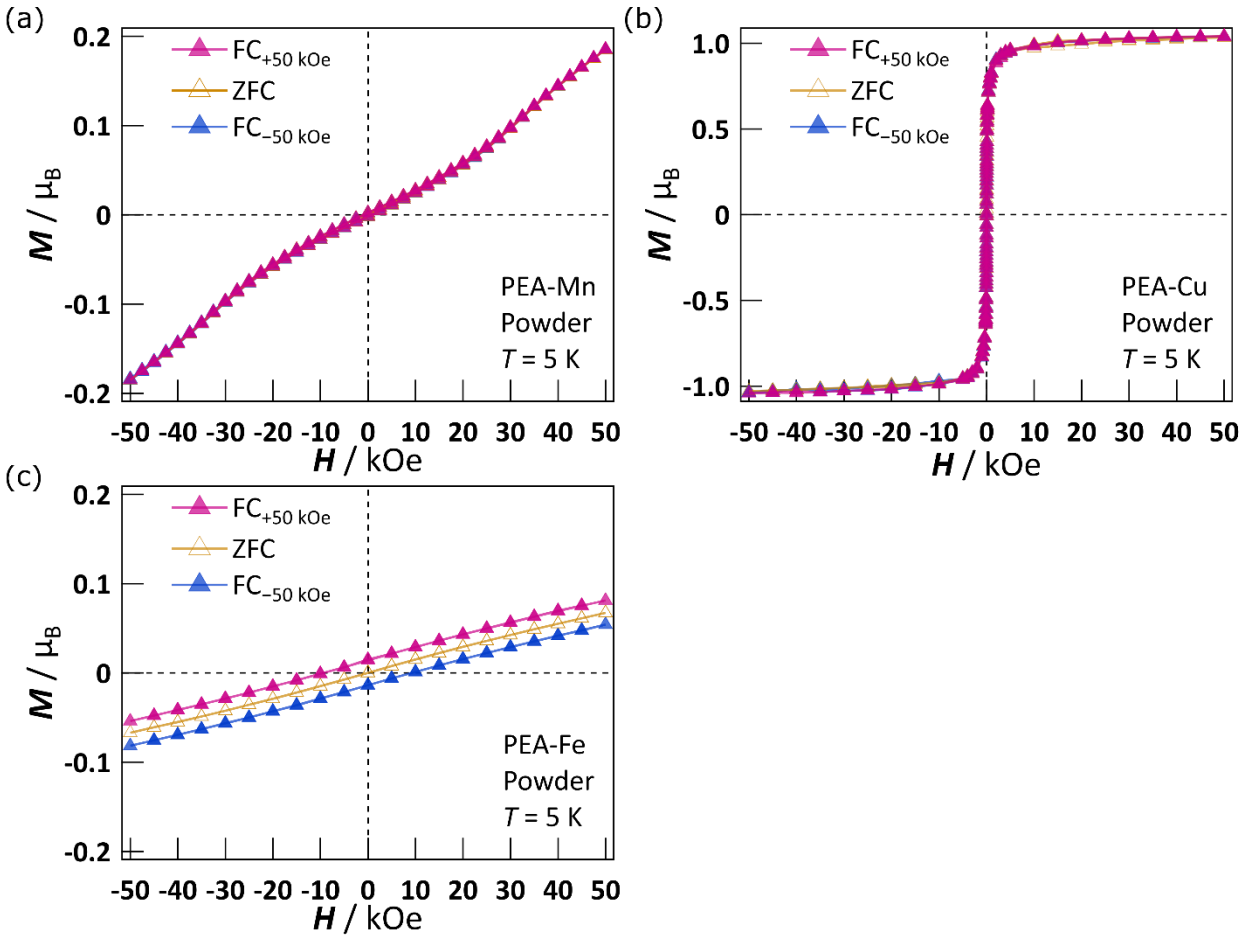

Fig. S6 Field-dependence of the magnetization for powder samples of (a) PEA-Mn, (b) PEA-Cu and (c) PEA-Fe after ZFC, FC_{+50kOe} and FC_{-50kOe}.

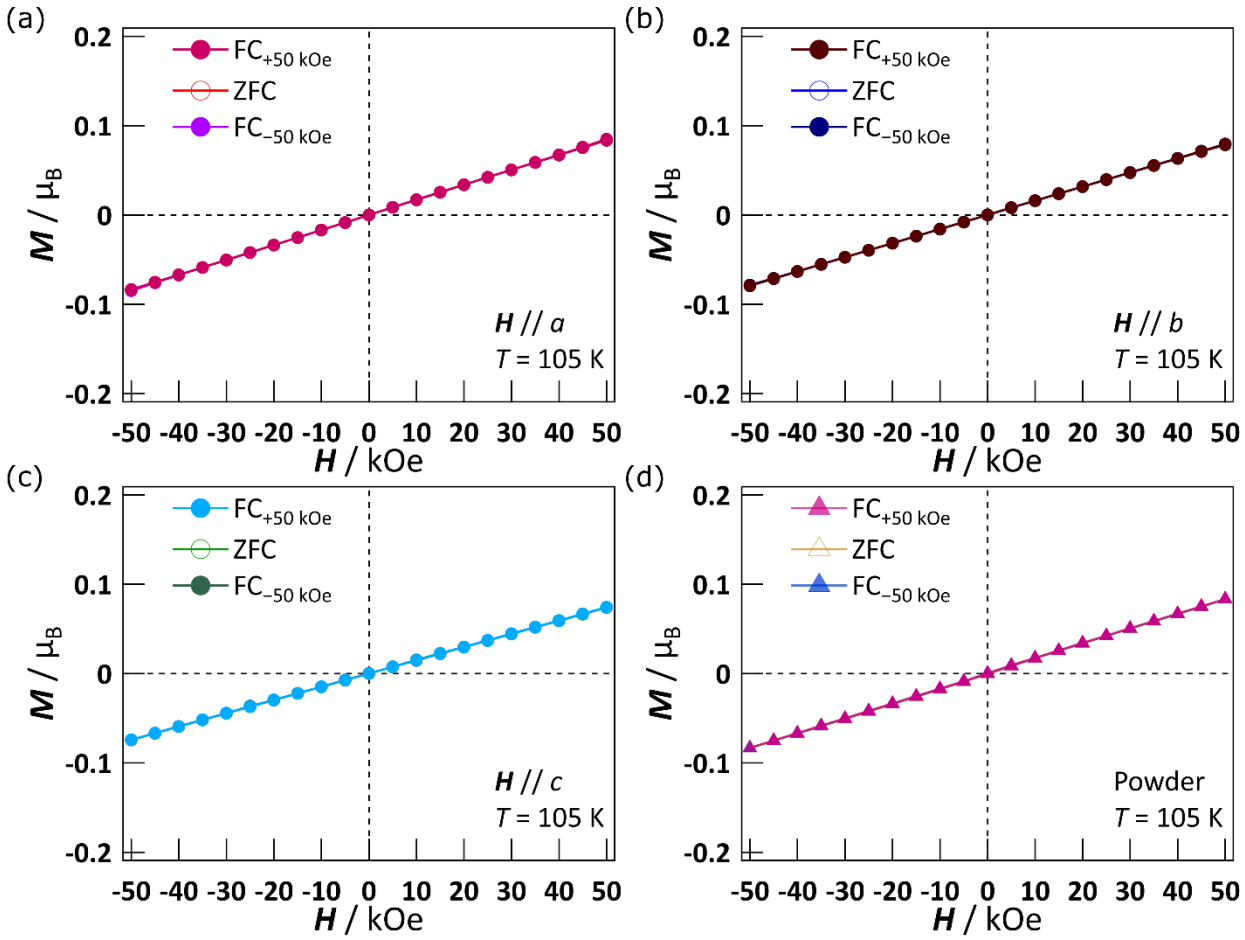

Fig. S7 Field-sweep measurements at 105 K for single crystal and powder samples of PEA-Fe after ZFC, FC_{+50kOe} and FC_{-50kOe}.

(a)$H \parallel a$ (b) $H \parallel b$ (c) $H \parallel c$ (d) Powder

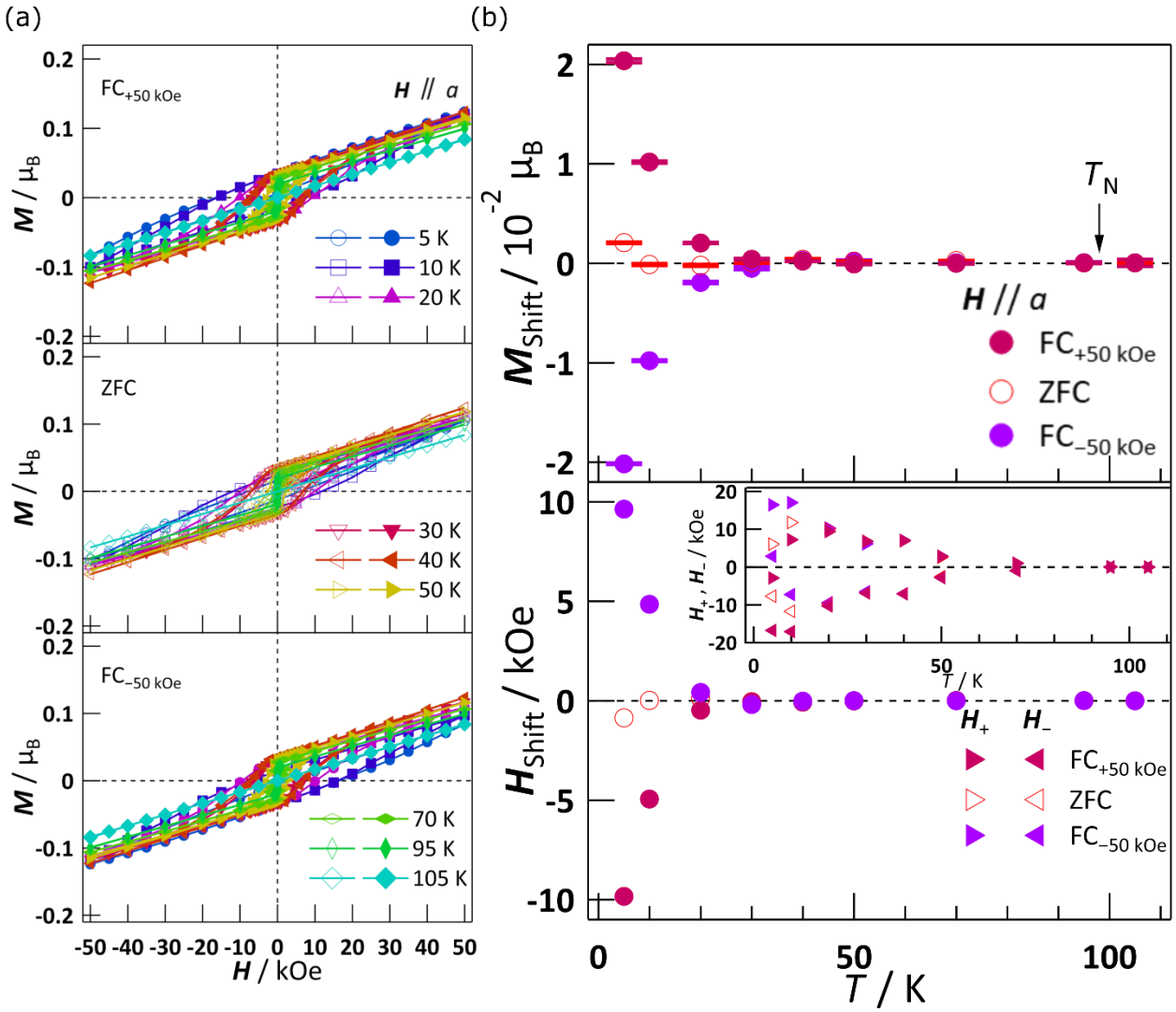

Fig. S8 (a) Field-dependences of magnetization for PEA-Fe along the *a*-axis at various temperatures after (top) FC_{+50kOe}, (middle) ZFC and (bottom) FC_{-50kOe}, respectively. (b) Temperature dependence of M_{Shift}, H_{Shift}, H_+ and H_- along the *a*-axis after ZFC and FC processes. M_{Shift} can be defined as $(M_+ + M_-)/2$, where M_+ and M_- are the magnetization at +50 and −50 kOe magnetic fields, respectively. Additionally, H_{Shift} is calculated using the equation $H_{Shift} = (H_+ + H_-)/2$, where H_+ and H_- correspond to the upper and lower magnetic fields at the magnetization of zero.

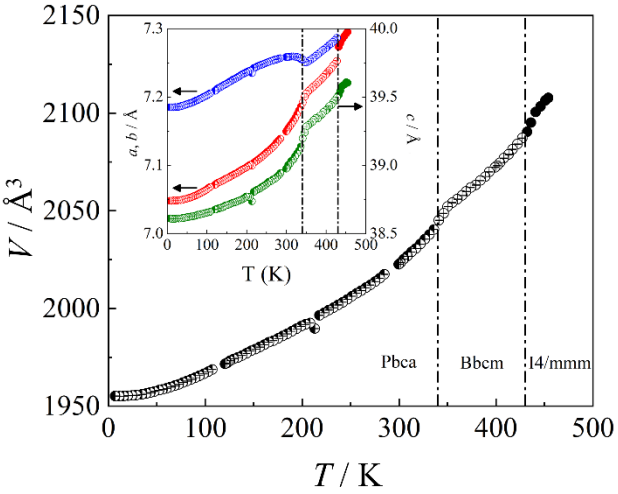

Fig. S9 Evolution of the unit cell volume and (inset) the lattice parameters as function of the temperature for PEA-Fe.

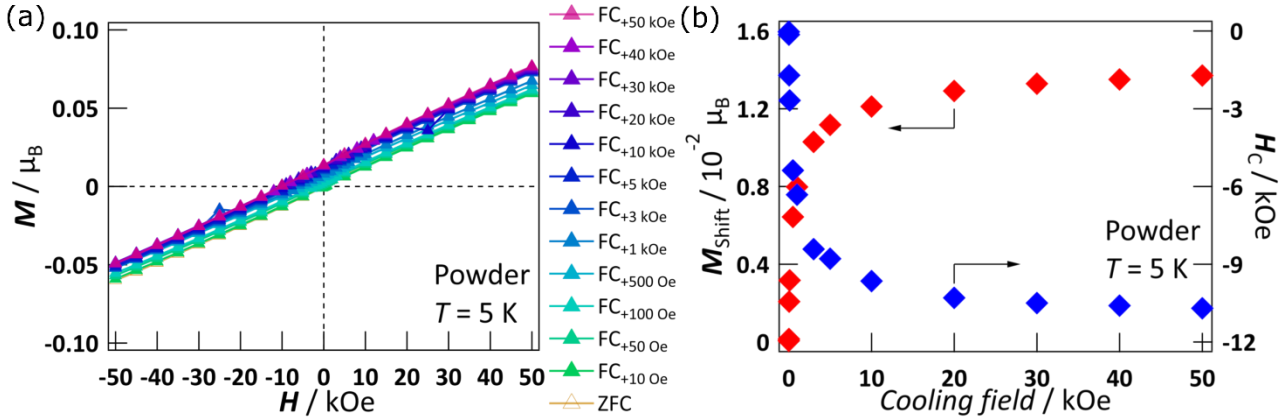

Fig. S10 (a) The field dependence of magnetization after various field cooling for powder sample of PEA-Fe. (b) The values of the magnetization shift (M_{Shift}) and the coercive field (H_C) as a function of the cooling field.

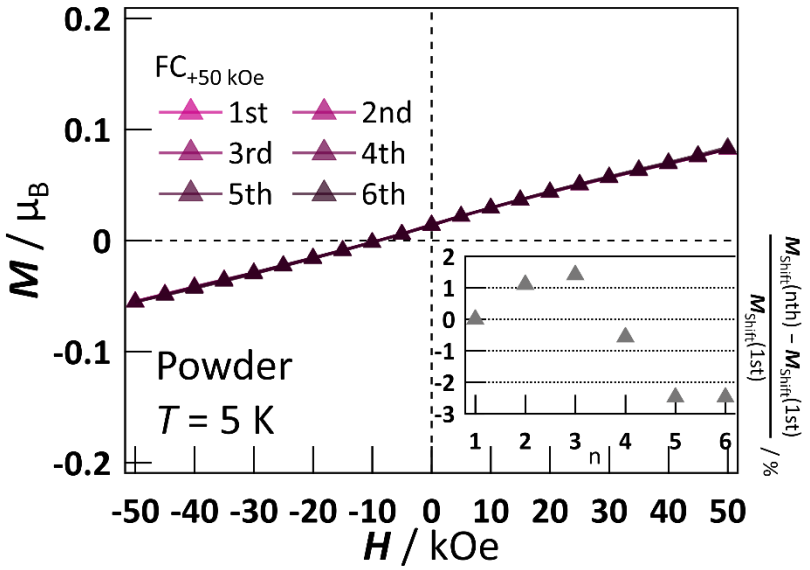

Fig. S11 The field dependence of magnetization over six measurement cycles for powder sample of PEA-Fe. The inset is the $[M_{shift}(nth) - M_{shift}(1st)]/M_{Shift}(1st)$ as a function of cycling number n

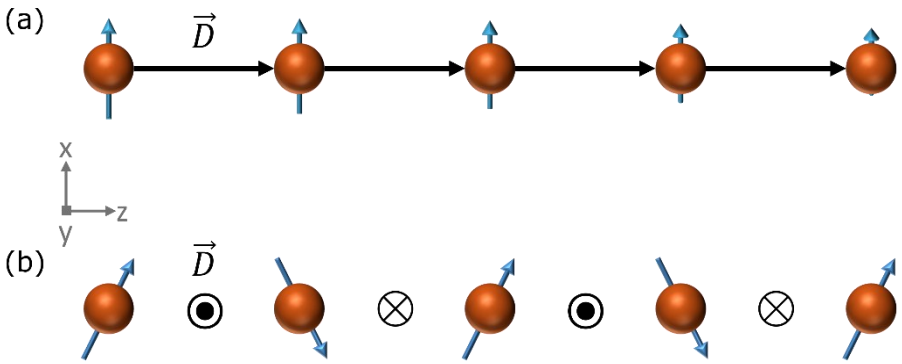

Fig. S12 Schematic picture of the direction of the DM vector ($\vec{D}$) in (a) chiral helimagnets and (b) canted antiferromagnets. The DM vectors are aligned along the z-direction in (a), while are anti-parallel to each other along the y-direction in (b).

Table S1. Summary of thermal analyses for PEA-*M* (*M* = Mn, Cu, Fe).

Compound	PEA-Mn	PEA-Cu	PEA-Fe[a]
Process	heating / cooling	heating / cooling	heating / cooling
Temperature / K	364 / 368	340 / 334	345 / 343
ΔH / kJ mol^{-1}	2.8 / 2.8	1.0 / 1.2	1.8 / 1.7
ΔS / J mol^{-1}	7.7 / 7.6	2.9 / 3.6	5.2 / 5.0
N	2.5 / 2.5	1.4 / 1.5	1.9 / 1.8
Temperature / K	415 / 418	408 / 409	433 / 433
ΔH / kJ mol^{-1}	2.0 / 2.1	2.4 / 2.3	0.9 / 0.9
ΔS / J mol^{-1}	4.8 / 5.0	5.9 / 5.6	2.1 / 2.1
N	1.8 / 1.8	2.0 / 2.0	1.3 / 1.3

[a] Y. Nakayama, S. Nishihara, K. Inoue, T. Suzuki and M. Kurmoo, *Angew. Chem. Int. Ed.*, 2017, **56**, 9367–9370.

Table S2. Crystallographic parameters of PEA-Mn at different temperatures.

Formula	$C_{16}H_{24}N_2MnCl_4$		
Formula weight	441.11		
Temperature / K	293	393	433
Crystal system	Orthorhombic	Orthorhombic	Tetragonal
Space group (no.)	*Pbca* (61)	*Bbcm* (64)	*I*4/*mmm* (139)
a / Å	7.2039(3)	7.2822(13)	5.16257(7)
b / Å	7.2919(3)	7.3039(13)	5.16257(7)
c / Å	39.3912(14)	39.910(7)	39.9478(12)
Volume / $Å^3$	2069.22(14)	2122.7(6)	1064.69(4)
Z	4	4	2
Density (cal.) / g cm^{-3}	1.416	1.380	1.376
Absorption coefficient / mm^{-1}	1.154	1.125	1.121
F(000)	908	908	454
Reflections collected	19429	10068	11678
Independent reflections	2357	1221	544
Goodness-of-fit on F^2	1.385	1.156	1.160
R_1 [$I > 2\sigma(I)$]	0.0565	0.0511	0.0335
wR_2 [all data]	0.1122	0.1323	0.1045
Largest diff. peak/hole / e $Å^{-3}$	0.70/−0.54	0.24/−0.45	0.30/−0.24

Table S3. Crystallographic parameters of PEA-Cu at different temperatures.

Formula	$C_{16}H_{24}N_2CuCl_4$		
Formula weight	449.72		
Temperature / K	293	393	433
Crystal system	Orthorhombic	Orthorhombic	Tetragonal
Space group (no.)	*Pbca* (61)	*Bbcm* (64)	*I*4/*mmm* (139)
a / Å	7.2924(8)	7.3448(2)	5.23790(10)
b / Å	7.3280(8)	7.3896(2)	5.23790(10)
c / Å	38.583(5)	39.0232(11)	39.1329(9)
Volume / $Å^3$	2061.8(4)	2117.99(10)	1073.63(5)
Z	4	4	2
Density (cal.) / g cm^{-3}	1.449	1.410	1.391
Absorption coefficient / mm^{-1}	1.577	1.535	1.515
F(000)	924	924	462
Reflections collected	20160	10175	21351
Independent reflections	2371	1247	435
Goodness-of-fit on F^2	1.323	1.097	1.197
R_1 [$I > 2\sigma(I)$]	0.0700	0.0393	0.0774
wR_2 [all data]	0.1792	0.1149	0.2170
Largest diff. peak/hole / e $Å^{-3}$	0.71/−1.25	0.30/−0.49	1.44/−1.60

Table S4. Crystallographic parameters of PEA-Fe at different temperatures.

Formula	$C_{16}H_{24}N_2FeCl_4$		
Formula weight	442.02		
Temperature / K	293	373	453
Crystal system	Orthorhombic	Orthorhombic	Tetragonal
Space group (no.)	*Pbca* (61)	*Bbcm* (64)	*I*4/*mmm* (139)
a / Å	7.1717(3)	7.2427(2)	5.17610(10)
b / Å	7.2827(3)	7.2798(2)	5.17610(10)
c / Å	39.0900(17)	39.4455(9)	39.7194(11)
Volume / $Å^3$	2041.64(15)	2079.78(9)	1064.16(5)
Z	4	4	2
Density (cal.) / g cm^{-3}	1.438	1.412	1.379
Absorption coefficient / mm^{-1}	1.262	1.239	1.21
F(000)	912	912	456
Reflections collected	18415	9468	10205
Independent reflections	2338	1214	433
Goodness-of-fit on F^2	1.465	1.067	1.204
R_1 [$I > 2\sigma(I)$]	0.0876	0.0443	0.0285
wR_2 [all data]	0.1935	0.1189	0.0891
Largest diff. peak/hole / e $Å^{-3}$	0.81/−0.77	0.34/−0.51	0.26/−0.16

Table S5. Structural parameters using neutron data for PEA-Fe determined at different temperatures in the *Pbca* space group phase.

Temperature / K	300	120	50	2
Space group	*Pbca*	*Pbca*	*Pbca*	*Pbca*
a / Å	7.1485(1)	7.07161(8)	7.05202(9)	7.04839(9)
b / Å	7.2584(1)	7.20907(9)	7.1895(1)	7.1848(1)
c / Å	38.974(1)	38.6736(8)	38.6241(8)	38.6133(9)
$\alpha = \beta = \gamma$ (º)	90	90	90	90
χ^2	11.61	26.6	32.0	36.2
R_{Bragg}	10.2	6.92	7.76	8.34
$R_{Magnetic}$	-	-	45.4	58.2
$\vec{m}_{Fe}$ // *b*-axis / μ_B	-	-	2.5(2)	2.6(2)
Fe 4b (0,0,1/2)	-	-	-	-
$U_{iso, Fe}$ (Å ^{2})	3.4(3)	0.1(2)	0.1(2)	0.2(3)
Cl1 8c (x,y,z)	0.011(2) 0.000(2) 0.4390(2)	0.023(1) 0.006(1) 0.4383(2)	0.021(1) 0.003(1) 0.4374(2)	0.022(1) 0.003(1) 0.4375(2)
$U_{iso, Cl1}$ (Å ^{2})	2.9(2)	0.7(1)	0.3(1)	0.3(1)
Cl2 8c (x,y,z)	0.249(2) 0.250(2) 0.5083(2)	0.245(1) 0.260(1) 0.5065(2)	0.246(1) 0.260(1) 0.5058(2)	0.247(1) 0.260(1) 0.5056(2)
$U_{iso, Cl2}$ (Å ^{2})	2.9(2)	0.7(1)	0.3(1)	0.3(1)
N 8c (x,y,z)	0.499(2) -0.003(1) 0.4431(2)	0.499(1) -0.007(1) 0.4429(2)	0.497(1) -0.006(1) 0.4432(2)	0.496(2) -0.006(1) 0.4433(2)
$U_{iso, N}$ (Å ^{2})	2.3(2)	0.4(2)	0.4(2)	0.4(2)
HNA 8c (x,y,z)	0.361(3) 0.026(8) 0.4538(9)	0.361(3) 0.026(3) 0.4538(5)	0.357(3) 0.013(4) 0.4546(5)	0.354(3) 0.004(4) 0.4557(5)
$U_{iso, HNA}$ (Å ^{2})	8.4(7)	0.9(4)	1.0(4)	1.0(4)
HNB 8c (x,y,z)	0.548(8)	0.548(3)	0.551(3)	0.551(3)

	0.110(3)	0.110(3)	0.119(3)	0.117(3)
	0.454(1)	0.4539(7)	0.4528(8)	0.4536(8)
$U_{iso, HNB}$ (Å ^{2})	8.4(7)	0.9(4)	1.0(4)	1.0(4)
	0.553(6)	0.553(3)	0.550(3)	0.550(4)
HNC 8c (x,y,z)	-0.138(4)	-0.138(3)	-0.136(3)	-0.138(3)
	0.452(1)	0.4522(7)	0.4533(8)	0.4523(8)
$U_{iso, HNC}$ (Å ^{2})	8.4(7)	0.9(4)	1.0(4)	1.0(4)
	0.540(2)	0.541(1)	0.540(2)	0.541(2)
C1 8c (x,y,z)	0.039(2)	0.032(2)	0.038(2)	0.037(2)
	0.4075(3)	0.4061(3)	0.4059(3)	0.4065(3)
$U_{iso, C1}$ (Å ^{2})	0.8(2)	0.2(2)	0.2(2)	0.2(2)
	0.685(3)	0.697(3)	0.701(3)	0.701(3)
H1A 8c (x,y,z)	0.052(5)	0.052(3)	0.048(4)	0.052(4)
	0.4082(8)	0.4103(6)	0.4105(7)	0.4105(7)
$U_{iso, H1A}$ (Å ^{2})	9.1(6)	0.9(4)	1.0(4)	1.0(4)
	0.544(5)	0.530(3)	0.524(4)	0.516(4)
H1B 8c (x,y,z)	0.182(3)	0.187(3)	0.194(3)	0.194(3)
	0.409(1)	0.4083(7)	0.4063(7)	0.4064(7)
$U_{iso, H1B}$ (Å ^{2})	9.1(6)	0.9(4)	1.0(4)	1.0(4)
	0.464(2)	0.464(2)	0.464(2)	0.464(2)
C2 8c (x,y,z)	-0.086(2)	-0.090(2)	-0.089(1)	-0.090(1)
	0.3833(3)	0.3796(3)	0.3783(3)	0.3778(3)
$U_{iso, C2}$ (Å ^{2})	0.8(2)	0.2(2)	0.2(2)	0.2(2)
	0.331(4)	0.310(3)	0.303(3)	0.301(3)
H2A 8c (x,y,z)	-0.125(4)	-0.115(3)	-0.109(3)	-0.106(3)
	0.3756(9)	0.3756(6)	0.3760(7)	0.3747(7)
$U_{iso, H2A}$ (Å ^{2})	9.1(6)	0.9(4)	1.0(4)	1.0(4)
	0.539(5)	0.530(3)	0.542(3)	0.545(4)
H2B 8c (x,y,z)	-0.214(4)	-0.222(3)	-0.226(3)	-0.226(3)
	0.381(1)	0.3803(6)	0.3766(6)	0.3766(7)
$U_{iso, H2B}$ (Å ^{2})	9.1(6)	0.9(4)	1.0(4)	1.0(4)

	0.487(3)	0.481(2)	0.482(2)	0.478(2)
C3 8c (x,y,z)	-0.022(3)	-0.031(2)	-0.030(2)	-0.030(2)
	0.3497(4)	0.3468(3)	0.3454(3)	0.3449(3)
$U_{iso, C3}$ (Å ^{2})	5.2(5)	0.7(3)	0.8(3)	0.9(3)
	0.359(3)	0.360(2)	0.361(2)	0.361(2)
C4 8c (x,y,z)	0.100(3)	0.111(2)	0.108(2)	0.110(2)
	0.3340(4)	0.3338(4)	0.3338(4)	0.3331(4)
$U_{iso, C4}$ (Å ^{2})	7.5(3)	0.8(1)	0.8(1)	0.6(1)
	0.253(7)	0.253(4)	0.246(3)	0.243(3)
H4 8c (x,y,z)	0.167(6)	0.167(3)	0.132(3)	0.143(3)
	0.342(1)	0.3424(6)	0.3437(8)	0.3439(7)
$U_{iso, H4}$ (Å ^{2})	8.4(6)	1.1(2)	1.2(3)	1.0(3)
	0.374(3)	0.378(2)	0.377(2)	0.379(2)
C5 8c (x,y,z)	0.145(3)	0.147(2)	0.150(2)	0.150(2)
	0.2988(4)	0.2963(3)	0.2977(3)	0.2964(3)
$U_{iso, C5}$ (Å ^{2})	7.5(3)	0.8(1)	0.8(1)	0.6(1)
	0.283(7)	0.283(3)	0.276(3)	0.273(4)
H5 8c (x,y,z)	0.263(7)	0.263(3)	0.258(4)	0.258(4)
	0.2920(9)	0.2920(5)	0.2913(6)	0.2906(6)
$U_{iso, H5}$ (Å ^{2})	8.4(6)	1.1(2)	1.2(3)	1.0(3)
	0.528(3)	0.529(2)	0.527(2)	0.534(2)
C6 8c (x,y,z)	0.088(2)	0.086(2)	0.088(2)	0.082(2)
	0.2768(4)	0.2721(3)	0.2733(3)	0.2727(3)
$U_{iso, C6}$ (Å ^{2})	7.5(3)	0.8(1)	0.8(1)	0.6(1)
	0.546(7)	0.546(3)	0.550(3)	0.543(3)
H6 8c (x,y,z)	0.151(4)	0.151(2)	0.163(3)	0.162(3)
	0.2547(7)	0.2547(6)	0.2551(6)	0.2541(7)
$U_{iso, H6}$ (Å ^{2})	8.4(6)	1.1(2)	1.2(3)	1.0(3)
	0.639(2)	0.641(2)	0.644(2)	0.645(2)
C7 8c (x,y,z)	-0.053(3)	-0.049(2)	-0.045(2)	-0.048(2)
	0.2909(4)	0.2900(3)	0.2899(3)	0.2908(4)

$U_{iso, C7}$ (Å ^{2})	7.5(3)	0.8(1)	0.8(1)	0.6(1)
	0.754(4)	0.754(3)	0.750(4)	0.754(3)
H7 8c (x,y,z)	-0.111(5)	-0.111(3)	-0.121(3)	-0.115(3)
	0.282(1)	0.2818(6)	0.2813(7)	0.2808(7)
$U_{iso, H7}$ (Å ^{2})	8.4(6)	1.1(2)	1.2(3)	1.0(3)
	0.619(3)	0.615(2)	0.620(2)	0.620(2)
C8 8c (x,y,z)	-0.101(3)	-0.108(2)	-0.112(2)	-0.110(2)
	0.3251(4)	0.3224(3)	0.3210(4)	0.3220(4)
$U_{iso, C8}$ (Å ^{2})	7.5(3)	0.8(1)	0.8(1)	0.6(1)
	0.710(6)	0.710(3)	0.704(3)	0.706(3)
H8 8c (x,y,z)	-0.189(7)	-0.189(3)	-0.214(3)	-0.210(4)
	0.330(1)	0.3297(6)	0.3249(6)	0.3237(6)
$U_{iso, H8}$ (Å ^{2})	8.4(6)	1.1(2)	1.2(3)	1.0(3)